Accepted Manuscript

Synthesis, structural characterization, in vitro cytotoxicities, DNA-binding and BSA interaction of diorganotin (IV) complexes derived from hydrazone Schiff base

Fei Wang, Handong Yin, Jichun Cui, Yanwei Zhang, Honglin Geng, Min Hong

PII: S0022-328X(13)00918-2

DOI: 10.1016/j.jorganchem.2013.12.037

Reference: JOM 18423

To appear in: *Journal of Organometallic Chemistry*

Received Date: 30 August 2013

Revised Date: 20 December 2013

Accepted Date: 21 December 2013

Please cite this article as: F. Wang, H. Yin, J. Cui, Y. Zhang, H. Geng, M. Hong, Synthesis, structural characterization, in vitro cytotoxicities, DNA-binding and BSA interaction of diorganotin (IV) complexes derived from hydrazone Schiff base, *Journal of Organometallic Chemistry* (2014), doi: 10.1016/j.jorganchem.2013.12.037.

Graphical Abstract-Synopsis

Synthesis, structural characterization, in vitro cytotoxicities, DNA-binding and BSA interaction of diorganotin (IV) complexes derived from hydrazone Schiff base

Fei Wang, Handong Yin*, Jichun Cui, Yanwei Zhang, Honglin Geng, Min Hong*

Shandong Provincial Key Laboratory of Chemical Energy Storage and Novel Cell Technology, School of Chemistry and Chemical Engineering, Liaocheng University, Liaocheng 252059, China

Synopsis

Five diorganotin(IV) complexes containing hydrazone Schiff base were synthesized and characterized. The in vitro cytotoxicities of two compounds as well as the ligand were investigated against several human cancer cell lines. Additionally, bioactivity mechanism such as DNA-binding and BSA-binding were explored via fluorescence spectra.

* Corresponding author. Tel.:/Fax: +866358239121.
E-mail address: handongyin@163.com (H.D. Yin); hongminlcu@163.com (M. Hong).

Graphical Abstract-Pictogram

Synthesis, structural characterization, in vitro cytotoxicities, DNA-binding and BSA interaction of diorganotin (IV) complexes derived from hydrazone Schiff base

Fei Wang, Handong Yin*, Jichun Cui, Yanwei Zhang, Honglin Geng, Min Hong*

Shandong Provincial Key Laboratory of Chemical Energy Storage and Novel Cell Technology, School of Chemistry and Chemical Engineering, Liaocheng University, Liaocheng 252059, China

Pictogram

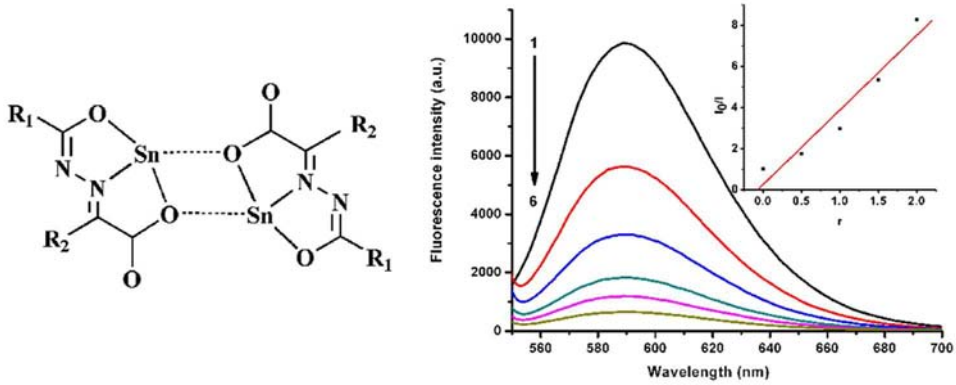

* Corresponding author. Tel.:/Fax: +866358239121.
E-mail address: handongyin@163.com (H.D. Yin); hongminlcu@163.com (M. Hong).

Highlight

1. Five diorganotin(IV) complexes were synthesized and characterized.
2. The cytotoxicities of two compounds and the ligand were tested by the SRB and MTT test.
3. Biological investigations like DNA binding and protein binding were carried out using two compounds by fluorescent spectra.

Synthesis, structural characterization, in vitro cytotoxicities, DNA-binding and BSA interaction of diorganotin (IV) complexes derived from hydrazone Schiff base

Fei Wang, Handong Yin*, Jichun Cui, Yanwei Zhang, Honglin Geng, Min Hong*

Shandong Provincial Key Laboratory of Chemical Energy Storage and Novel Cell Technology, School of Chemistry and Chemical Engineering, Liaocheng University, Liaocheng 252059, China

Abstract

Five diorganotin(IV) complexes of benzoylformic acid 3-hydroxy-2-naphthoyl hydrazone, $[R_2SnLY]_2$ (L = *3-HO-*$C_{10}H_6CON_2C(C_6H_5)CO_2$) with Y = H_2O, R = CH_3 (**1**), Y = EtOH, R = Ph (**3**), Y = EtOH, R = *o*-Cl-Bz (**4**), Y = EtOH, R = *o*-F-Bz (**5**), and $[R_2SnLY]$ with Y = EtOH, R = *n*-Bu (**2**) were prepared, which were structurally characterized by X-ray crystallography, elemental, IR and NMR (^{1}H and ^{13}C) spectroscopy. Structural analysis reveal that the ligand presents as tridentate ligand with ONO donors and coordinates to the tin center in an enolic form. Compound **2** is a monomer while the other compounds are weakly-bridged dimers with weak Sn···O interactions. In vitro cytotoxicities of compounds **1**, **3** and the ligand were determined to explore their potential anticancer activities. DNA binding properties of **1** and **3** with calf thymus DNA (ct-DNA) were investigated by fluorescence quenching method with ethidium bromide (abbr. EB)-DNA system. Furthermore, the protein fluorescence quenching studies reveal that there are strong binding interactions between compounds **1**，**3** and bovine serum albumins (BSA). Synchronous fluorescence spectra shows both the tryptophan and tyrosine residues in BSA are affected by the two compounds.

Keywords: Diorganotin(IV); Hydrazone; Crystal structure; Cytotoxicity activity; DNA-binding; BSA-binding.

1. Introduction

The quest for alternative drugs to the well-known cisplatin and its derivatives, which are still used in more than 50% of the treatment regimes for patients suffering from cancer, is highly needed [1,2].

* Corresponding author. Tel.:/Fax: +866358239121.
E-mail address: handongyin@163.com (H.D. Yin); hongminlcu@163.com (M. Hong).

These platinum compounds suffer from two main disadvantages: inefficient against platinum-resistant tumors and severe side effects. Furthermore, as a consequence of its particular chemical structure, cisplatin in particular offers little possibility for rational improvements to increase its tumor specificity and thereby reduce undesired side effects [3]. Hence, attempts are being made to replace cisplatin with suitable alternatives and numerous metal-based complexes have been synthesized and tested for their anticancer activities. Among them, organotin complexes show promising antitumor activities against a wide panel of tumors or tumor cell lines and many organotin complexes were screened against a variety of cell lines and were found to be active both in vitro and in vivo [4-8]. A. Alama and his coworkers investigated the cytotoxicities of tri-*n*-butyltin(IV) lupinylsulfide hydrogen fumarate in vitro and antitumor activity in vivo [9]. X.M. Shang prepared a serial of organotin carboxylates and reported their relationship between their properties (electrochemical behavior, structural rearrangements) and antitumor activities [10]. Another two di-*n*-butyltin(IV) derivatives synthesized by X.M. Shang were reported to displayed an arrest in the G0/G1 phase and a decrease of S phase of the cell cycle in KB cells at low concentrations of the two complexes [11]. Recent studies demonstrated that some tri- and diorganotin(IV) complexes were selectively mediated through the induction of apoptosis [12].

Hydrazone attracted special attention from researchers due to their well-known chelating capability and structural flexibility that can provide rigidity to the skeletal framework of the prepared metal complexes [13-15]. Based on the chelating ability, certain hydrazones were synthesized and applied in the treatment of iron over-loaded diseases, such as β-thalas semia major [16]. Fascinating chemical behaviors and biological essentialities such as antibacterial, antiproliferative, antimalarial and antitumor were also favored by researchers in the area of medicine and drugs. One ortho-hydroxy N-acyl hydrazone was reported to enhance the enzymatic activity of procaspase-3 in vitro and induce apoptosis in cancer cells [17]. A number of hydrazones such as 311 and PIH have been shown to have anti-proliferative activities [18, 19]. J.Q. Tong synthesized one hydrazone and studied the BSA binding abilities of the hydrazone employing several different techniques [20]. Meanwhile, large numbers of hydrazone-containing metal chelates were also synthesized. M. Alagesan and co-workers reported the synthesis, crystal structure and biological properties (DNA-bind, BSA-bind and in vitro cytotoxicities) of two copper(II) hydrazone complexes [21]. D.S. Raja synthesized a water soluble cobalt(II)-hydrazone polymer and investigated the DNA binding, protein interaction, radical scavenging

as well as anticancer activity of the complex [22]. E. Ramachandran and co-workers reported five thiosemicarbazone ligands and their corresponding palladium(II) complexes [23]. Besides, hydrazone Schiff bases were widely used as fluorescent probes for their fluorescence [24].

Though the exact antitumor mechanism presented by the mental-based anticancer agents remains unknown, lots of studies show that many anticancer agents could bind or cleave DNA. DNA is viewed as one of the main molecular targets in the design of anticancer compounds [25]. Organotin compounds are important species among these anticancer drugs which could interact with DNA. Our study found organotin complexes containing Schiff base could interact with CT-DNA through intercalation with different extent [26]. Besides, the interaction between anticancer agents and serum albumins which involved in the transport of metal ions and metal complexes through the blood stream are also widely investigated [27,28]. Because the nature and magnitude of drug–albumin interactions could influence the pharmacokinetics of drugs significantly. Further, it has been demonstrated that free radicals can damage proteins, lipids, and DNA of bio-tissues, leading to increased rates of cancer and fortunately antioxidants can prevent this damage due to their free radical scavenging activity [29]. Thus, radical scavenging is viewed as another property to be measured on anticancer agents. Despite the wealth of information available on these topics, limited reports are available on the related organotin complexes. Hence, in view of the great potential of hydrazone in drug design and the remarkable anticancer performance of organotin(IV) species, the synthesis, structural characterization, in vitro cytotoxicity, DNA and BSA interaction investigations of a series of organotin complexes with hydrazone are reported here and demonstrate a huge potential of this type of organometallics in medicinal chemistry.

2. Results and Discussion

2.1. Syntheses of diorganotin(IV) compounds

Complexes **1**–**5** were obtained by the reaction of the ligand/R_2SnCl_2/EtONa in a 1:1:2 molar ratio in ethanol/toluene (1:1) under refluxing. The synthetic procedures are shown in Scheme 1.

2.2. Spectroscopic data

Comparing the IR spectra of the complexes with the free ligand, a remarkable difference is the complete disappearance of C=O stretching frequencies (1649 cm^{-1}), which confirms that the ligand coordinates with the tin in the enolic form. The frequency separation between asymmetric stretching

vibration and symmetric stretching vibrations of COO lies between 230 and 282 cm^{-1} for compounds **1**-**5,** indicating the monodentate coordination mode of carboxylate group [29]. This is in accordance with the X-ray structure analysis. Strong bands at region 650-600 cm^{-1} in compounds **1**, **3**, **4** and **5** are assigned to a bridge Sn-O-Sn [30]. New bands at 470–481 cm^{-1} are characteristic of Sn–N absorption, respectively [31].

In the ^{1}H NMR spectra of free ligand, single resonance for COOH group is observed at δ = 13.38 ppm. The absent of COOH group in the ^{1}H NMR spectra of compounds **1**-**5** indicates the deprotonation of COOH group. The values are consistent with those reported for other $R_2Sn(O_2CR')_2$ systems [32,33]. Signal of -NH- could not be found in the ^{1}H NMR spectra of compounds **1**-**5**, suggesting the coordination to the central tin atom in the enolic form. Signal resonance for naphthoic hydroxyl can be observed at 10.83-12.33 ppm in all complexes which strongly suggests that the naphthoic hydroxyl oxygen atom does not participate in coordination to the tin atom. Comparing with the ligand, the ^{13}C NMR values of COO, CONH shift to downfield about 8 ppm and 3 ppm due to the coordination of COOH and -NH- groups, while there is only little downfield of C=N and C-OH groups. The shift is a consequence of an electron density transfer from the ligand to the acceptor. The δ values of naphthoic hydrogens and carbons are consistent with those reported values[34,35].

2.3. X-ray crystallography

*2.3.1. X-ray crystallography of complexes **1**, **3**, **4** and **5**.*

The molecular structures of the compounds **1**, **3**, **4** and **5** are illustrated in Fig. 1, respectively. Crystal data are listed in Table 1. Selected bond distances and angles are listed in Table 2. We take complex **1** as an example to describe their structural characteristics.

In complex **1**, the Sn atom exists in a distorted pentagonal–bipyramidal configuration, being coordinated by three O atoms and one N atom from the ligand, one O atom from the water molecule and two C atoms from trans alkyl groups. The axial C(20)-Sn(1)-C(21) angle is not 180º but 166.0(2)º, which proves the distortion of the geometry. Atom O(1) of the carboxylate residue also binds more weakly to the other Sn atom, Sn^{i}, generating an Sn_2O_2 four-membered ring [symmetry code: -x, -y+1, -z+1]. The sum of the angles subtended at the Sn atom in the equatorial plane is typical for the ideal value of 360.01º for complex **1** for Sn(1), so that the Sn(1), O(1), N(1), O(3), O1#1and O(5) atoms are almost in the same plane. The distance of Sn(1)-O(1)#1 [2.661(3)Å] is longer than the sum of the

covalent radii of Sn and O (2.56Å), but is signficantly shorter than the sum of the van der Waals radii of tin and oxygen (3.68Å). Such Sn···O bond should be considered as weak bonding interaction. The Sn(1)-O(5) bond length is 2.373(3)Å and is longer than those analogous complexes [29,36] which can be attributed to the formation of intramolecular hydrogen bonds (O5-H5···O2#1). The distance of Sn(1)-O(3) [2.216(3)Å] is shorter than the sum of the covalent radii of Sn and O (2.56Å), indicating strong Sn···O interaction. The Sn(1)-N(1) distance [2.299(4) Å] is a little longer than the sum of the covalent radii of Sn and N (2.15 Å). As described above, structure of compound **1** can be described as weakly-bridged dimers with weak Sn···O interactions and the coordination geometries of tin atom can also be described as trans-C_2SnO_4N pentagonal bipyramid with two alkyl groups occupying trans positions. Undoubtedly, intramolecular and intermolecular hydrogen bonds observed in compound **1** contribute to the stability and compactness of the dimmer (Table 4).

The bond length of C(9)-O(3) [1.270(5)Å] lie between double (1.224Å) and single-bond (1.430Å) lengths. Compared with the length of a C=N double bond (1.38Å) and a C-N single bond (1.470Å), C(9)-N(2) [1.345(5)Å] bond as well as C(2)-N(1) [1.292(5)Å] should be classified as C=N double bonds. N(1)-N(2) bonds [1.378(5)Å] fall within the normal range of N-N single-bond [37,38]. These data indicate that a C=N-N=C conjugated system is introduced into the inner coordination sphere and the ligand functions as a tridentate chelate with ONO donors. Additionally, the tridentate ligand forms two five-membered chelate ring with the central Sn atom, which contribute to the stability of the crystals.

As for complexes **3**, **4** and **5,** the coordination environment is similar to complex **1.** The axial angle is 171.66(12)º, 161.85(18)º and 163.2(3)º for complexes **3**, **4** and **5,** respectively. Atom O1 of the carboxylate residue binds more weakly to the other Sn atom, Sn^i, generating an Sn_2O_2 four-membered ring [symmetry code: (**3**) -x+2, -y+1, -z; (**4**) -x, -y, -z+1; (**5**) -x+1, -y+1, -z] with the distance of Sn1-O1#1[**3:** 2.581(2)Å; **4**: 2.628(3)Å; **5**: 2.638(4)Å]. The Sn(1)-O(3) bond lengths [2.182(2)Å for **3**, 2.162(3) Å for **4** and 2.181(4) Å for **5**] are shorter than the bond lengths observed in complex **1.** As for Sn(1)-N(1) bond length, complex **4** shows the shortest length with 2.244(3) Å, while complex **4** shows the longest bond length of Sn(1)-O(5) [2.428(3) Å]. The Sn(1)-O(1) varies from 2.349(3) Å (complex **4**) to 2.393(4) Å (complex **5**). Other bond lengths such as C(9)-O(3), C(9)-N(2), C(2)-N(1) and N(1)-N(2) are similar to complex **1.** Hydrogen bonds [O(4)-H(4)···N(2) and O(5)-H(5)···O(2)#1] can be observed in complexes **3**, **4** and **5.**

*2.3.2. Crystal structure of complex **2***

For compound 2, the molecular structure is best described as monomer due to the long distance of Sn(1)-O(1)#1 [2.819(4)Å, #1: 1-x, 2-y, -z]. The Sn atom adopts a six-coordinate geometry, with the equatorial positions occupied by three oxygen atoms [O(1), O(3), O(5)] and one nitrogen N(1) (Fig. 2). The Schiff base coordinates to the Sn atom as a tridentate ligand via the azomethine N atom, the hydroxyl O atom and the carbonyl O atom. The O atoms from the ligand coordinate to the Sn atom with one short [Sn(1)-O(3) 2.175(4) Å] and one long Sn-O bond [Sn(1)-O(1) 2.304(4) Å]. Atoms O(1), O(3), O(5) and N(1) are coplanar with angles subtended at the Sn atom in the equatorial plane is 360.02º. The axial angle C(21)-Sn(1)-C(24) [162.5(4)º] deviates from the ideal value of 180º (Table 3). Thus the coordination environment is a distorted octahedral geometry. The bond length of C(9)-O(3), C(9)-N(2) as well as C(2)-N(1) are similar to the above complexes. Hydrogen bonds can also be observed in compound **2** (Table 4).

2.4. In vitro cytotoxicities activity

The in vitro cytotoxicities of complexes **1**, **3** and the free ligand were determined by SRB and MTT-based assay to understand the possible relationship between the different tin(IV) moieties (bearing dimethyl and diphenyl groups), the ligand and the cytotoxicities activity. Complexes were tested for cytotoxicities activity on seven tumor cell lines: human lung cancer cell line (A549), human hepatocellular carcinoma cell line (SMMC-7721), murine leukemia cell line (P388), human colon carcinoma (WiDr), human colon cell line (HCT-116) and non-cancer cell human umbilical vein endothelial cells (HUVEC). The results are expressed as IC_{50} (in μg/ml) and the corresponding IC_{50} values are listed in Table 5. Possible structure-activity relationships could be recognized as follows:

(1) Diphenyl (IV) compound **3** was more potent than dimethyltin compound **1** in inhibiting the growth of most of the cell lines tested here. Complex **3** is the most efficient antitumor agent for SMMC-7721, A549, P388, HCT-116 and HUVEC cells while complex **1** exhibits the highest activities against WiDr cells. Among them, the most outstanding result is obtained from the activity of complex **3** in HCT-116 tumor cells (4.00 μg/ml). Besides, the ligand exhibit almost non-inhibition for cellular proliferation. As far as one complex concerned, every organotin complexes tested here showed some degree of selectivity toward the seven tumor lines. Take compound **3** for example, about 4-fold improvement of the antitumor potency in HCT-116 cells compared to Caco-2 cells, 2-fold improvement

in SMMC-7721 cells than A549 cells.

(2) Every tumor cell line reported here exhibits different resistance to different organotin compounds. A549 cells exhibit somewhat low sensitivity to both complexes. WiDr cells show similar moderate resistance and SMMC-7721, HCT-116 and P388 cells exhibit high sensitivity. Compared to compound **3,** compound **1** is less toxic toward non-cancer cell (HUVEC).

(3) Analyses of crystal structures of **1** and **3** demonstrate that they have similar coordination geometry. Changes of the organic group result in different inhibition for the same cancer cell. In our experiments, complex **3** shows the antitumor effect of 4.24, 3.38 and 2.58 times more potent than complex **1** in HCT-116, SMMC-7721 and P388 cell lines, respectively. To some extent, our results are in accordance with the previous studies [8,9,39].

2.5. Fluorescence spectra

The interaction of complexes **1** and **3** with DNA has been evaluated by the ethidium bromide (abbr. EB)-DNA system with limited EB bound to excess of DNA, which can be used to distinguish intercalating and non-intercalative ligands [40]. Competitive binding of other intercalators leads to a loss of fluorescence because of depletion of the EB-DNA complex [40,41]. As shown in Fig. 3, the fluorescent intensity of EB in the bound form is remarkably quenched upon adding organotin complexes and a dose-response phenomenon is observed. However, complex **1** causes the lower fluorescence value to decrease, indicating lower DNA-binding ability. According to the classical Stern–Volmer equation:

$I/I_0 = 1 + K_{sq}r$

where I_0 and I represent fluorescence intensities in the absence and presence of the samples, respectively; r corresponds to the concentration ratio of the sample to DNA. K_{sq}, the linear Stern–Volmer constant, can be obtained from the slope of I_0/I versus r linear plot. From the insets in Fig. 3, the values of K_{sq} for **1** and **3** can be calculated as 0.2372 and 3.626, respectively, indicating stronger interaction between complex **3** and DNA. The quenching plot of **1** is in good agreement with the linear Stern–Volmer equation and can be defined as intercalative mode with DNA. Compared with **1**, the exact interaction between DNA and **3** can be more complicated since the linear relationship is not well presented and may exist other interactions between **3** and DNA. To some extent, this result can partly explain the cytotoxicities of the two complexes for the same cancer cell. Organotin complex **3** with stronger DNA-binding ability exhibited higher cytotoxic activity in SMMC-7721, A549, P388 and

HCT-116 cells possibly due to their ability to interact with DNA.

2.6. Protein binding studies

2.6.1.Fluorescence Quenching Studies.

The interaction of diorganotin(IV) complexes (**1** and **3)** with BSA is monitored by studying the quenching of the fluorescence of BSA with increasing concentration of organotin(IV) complexes. Tryptophan residue makes major contribution to the intrinsic fluorescence of protein. The emission is sensitive to the changes in the local environment of the tryptophan and can be attenuated by binding of a small molecule at or near this residue. As can be seen from Fig. 4 and Fig. S2(A), the fluorescence intensities of the protein are decreased regularly with increasing concentration of the probe compounds, indicating the binding of complexes to the protein. Addition of the compounds to BSA resulted in a significant decrease in the fluorescence intensity of BSA at 344 nm, up to 47.78 and 46.79 % of the initial fluorescence intensity of BSA accompanied by a hypsochromic shift of 4 and 2 nm for complexes **1** and **3**, respectively. Commonly, fluorescence quenching can be described by the following Stern−Volmer equation :

$$I_0/I = 1 + K_{sv}[Q] = 1 + k_q\tau_0[Q].$$

where I_0 and I are the steady-state fluorescence intensities in the absence and presence of quencher, respectively, K_{sv} is the Stern−Volmer quenching constant, [Q] is the total concentration of quencher, k_q is the bimolecular quenching constant, and τ_0 is the average lifetime of protein in the absence of quencher, and its value is 10^{-8} s [43]. K_{sv} can be obtained by a slope from the plot of F_0/F vs. [Q] (Fig. 5A and Table 6). All plots represent a good linear relationship, indicating a single quenching mechanism, either static (the formation of a complex between quencher and fluorophore) or dynamic (a collisional process) [44]. The K_q values (~10^{13} M^{-1} s^{-1}) of the complexes **1** and **3** are higher than the maximum scatter collision-quenching constant of diverse kinds of quenchers for biopolymers fluorescence (2×10^{10} M^{-1} s^{-1}) indicating the existence of static quenching mechanism [45]. Based on the plot of log (I_0-I)/I versus log [Q] (Fig. 5B), the number of binding sites [(n = 1.237 (complex **1**), 1.162 (complex **3**)] and binding constant [K_{bin} = 1.72×10^6 M^{-1}(**1**), 6.82×10^5 M^{-1} (**3**)] can been obtained. The values of K_q and K_{bin} indicate strong interaction between the BSA protein and the two organotin complexes, suggesting they can easily be stored in protein.

2.6.2. Characteristics of the synchronous fluorescence spectra

Structural changes of BSA particularly the vicinity of the fluorophore groups induced by compounds can be reflected by the synchronous fluorescence spectra of BSA. The synchronization fluorescence spectrum has been reported to be an effective approach to distinguish the tryptophan (Trp) ($\Delta\lambda$ = 60 nm) and tyrosine (Tyr) ($\Delta\lambda$ =15 nm) residues in protein [46]. The effect of organotin complexes on BSA synchronous fluorescence spectroscopy with $\Delta\lambda$ = 15 nm and $\Delta\lambda$ = 60 nm are shown in Fig. 4 and Fig. S2, respectively. According to the above result, two diorganotin complexes demonstrate similar BSA binding ability and now they show similar synchronous spectroscopy. Take complex **3** for example, in the synchronous fluorescence spectra of BSA at $\Delta\lambda$ = 15 nm, additions of the complex **3** result in a decrease of BSA at 282 nm, up to 72.9% of the initial fluorescence intensity with no shift in their emission wavelength maxima. On the other hand, in the case of $\Delta\lambda$ = 60, a decrease of up to 52.6 % at 282 nm of the initial fluorescence intensity of BSA accompanied with a blue shift of 2 nm could be observed. The above results suggest that the fluorescence intensity of both tryptophan and tyrosine residues of BSA are affected but to the larger extent in the case of former by the complexes.

3. Conclusions

A series of diorganotin(IV) compounds, bearing benzoylformic acid 3-hydroxy-2-naphthoyl hydrazone, are isolated and structurally characterized. For **1**, **3**, **4** and **5**, all complexes present as centrosymmetric dimeric structures with weak Sn¨O interactions while complex **2** presents as a monomer. For **1** and **3**, change of the organo group leads to different inhibitions for the same tumorigenic cells. Complex **3** is highly active against two tumor cell lines (SMMC-7721 and HCT-116), whereas complex **1** shows the lowest IC_{50} on WiDr cells. Fluorescence spectra reveal that complex **3** exhibits stronger DNA-binding ability than complex **1.** BSA-binding properties investigations reveal that complexes **1** and **3** exhibit similar strong binding ability toward BSA, suggesting these compounds can easily be stored in protein. Synchronous fluorescence spectra show both the tryptophan and tyrosine residues in BSA are affected by the two compounds.

4. Experimental details

4.1. Materials and measurements

Dimethyltin dichloride, di-*n*-butyltin dichloride and diphenyltin dichloride were commercially available and they were used without further purification. Di-*o*-chlorobenzyltin chloride and

di-*o*-fluorobenzyltin chloride were prepared by the methods reported in the literature [47]. Analytical grade solvents used in this work were undried. Elemental analyses were performed on a PE-2400-II elemental analyzer. IR spectra were recorded on a Nicolet-5700 spectrophotometer using KBr discs. ^{1}H, and ^{13}C NMR spectra were recorded on a Varian Mercury Plus-400 NMR spectrometer. Chemical shifts were given in ppm relative to Me_4Si(^{1}H, ^{13}C) in $CDCl_3$ or DMSO solvent. UV-vis was performed on a UV-2550 ultraviolet spectrophotometer. Fluorescence spectra were recorded on a F-7000 FL spectrophotometer.

4.2. Determination of crystal structures

Diffraction data for **1-5** were obtained on a Bruker Smart 1000 CCD diffractometer (graphite mo nochromated Mo-Ka radiation, λ= 0.71073 Å). All data were corrected using SADABS and the final refinement was performed by full-matrix least-squares with anisotropic thermal parameters for non-hydrogen atoms on F^2 using SHELX-97. The hydrogen atoms were added theoretically, riding on the concerned atoms and refined with fixed thermal factors. The carbons (C32) of an ethanol in **3** and the atoms (C28, C29, C30, C31, C32, C33, C34, C35, F1, F2) of one di-*o*-fluorobenzyl group in **5** were disordered. The site occupation factors of these disordered atoms were adjusted (0.5 for each atom) to give reasonable thermal parameters.

4.3. Preparation of Schiff base ligand

20 mL ethanol solution of 2-picolinic acid (10 mmol, 1.23 g) was added dropwise to an ethanol solution (40 mL) containing 3-hydroxy-2-naphthoic acid hydrazide (10 mmol, 2.02 g). The mixture was heated under reflux with stirring for 3 h. The crude product was precipitated when the solution cooled down. Then the product was filtered and washed with ethanol for three times. Yield: 88%, M.p. 199~200 °C. Anal. Calc. for $C_{19}H_{14}N_2O_4$ (334.33): C: 68.26; H: 4.22; N: 8.38 %； found C: 68.35; H: 4.25; N: 8.34 %. IR (KBr, cm^{-1}): 3413 (s, NH); 3252 (s, COOH); 1649 (s, C=O); 1596 (s, C=N). ^{1}H NMR (*d*-DMSO, ppm): 13.37 (s, 1H, COOH), 11.74 (s, 1H, OH), 11.45 (s, 1H, NH), 8.68(s, 1H, H_1)，7.95(d, 1H, J=4 Hz, H_8), 7.77(d, 2H, J=4 Hz, H_{12}), 7.72(d, 1H, J=8Hz, H_5), 7.52-7.44(m, 3H, H_{13}, H_{14}), 7.36-7.33 (m, 2H, H_6, H_7). 7.20(s, 1H, H_4),^{13}C NMR (*d*-DMSO, ppm): 164.4(COOH), 162.6(C=N), 153.3(C^3), 144.3(CONH), 136.8(C^{10}), 135.0(C^{11}), 134.0, 130.2, 129.8, 129.2, 129.0, 128.5, 127.9, 126.3, 124.6(C^7), 120.9(C^2), 111.3(C^4).

4.4. Syntheses of complexes 1–5

The complexes were prepared under nitrogen atmosphere. Benzoylformic acid 3-hydroxy-2-naphthoyl hydrazone (0.334g, 1.0 mmol), EtONa (0.136g, 2.0 mmol) were added to a stirred solution of 30 mL ethanol/toluene (1:1) in a round bottomed flask and stirred for 0.5 h. Dialkylltin dichloride (1.0 mmol) was then added to the reactor. The reaction mixture was stirred and heated at reflux for 8 h and then filtrated. The filtrate was evaporated in vacuum. The obtained solid was recrystallized from dichloromethane/ethanol (1:1). Yellow block crystals were slowly formed at room temperature.

4.4.1. {$Me_2Sn[3\text{-}HO\text{-}C_{10}H_6CON_2C(C_6H_5)CO_2](H_2O)\}_2$ ***(1)***

Yield: 63%, M.p.: >300 °C. Anal. Calc. for $C_{42}H_{40}N_4O_{10}Sn_2$: C, 50.54; H, 4.04; N, 5.61%. Found: C,50.78; H, 4.08; N,5.72%. IR (KBr, cm^{-1}): 3432 (m, H_2O); 1641 (s, $\upsilon_{as}COO$); 1388 (s, υ_sCOO); 1576 (m, C=N-N=C); 631 (s, Sn-O-Sn); 525 (w, Sn-C); 475 (m, Sn-N). ^1H NMR (*d*-DMSO, δ ppm): 12.33 (s, 1H, Ar-OH), 8.53(s, 1H, H_1), 7.84(d, 1H, J=8 Hz, H_8), 7.73(d, 2H, J=8 Hz, H_{12}),7.63(d, 1H, J=8 Hz, H_5), 7.53-7.50(m, 3H, H_{13}, H_{14}), 7.42(t, 1H, J=8 Hz, H_6), 7.26(t, 1H, J=8 Hz, H_7), 7.10(s, 1H, H_4), 3.38 (s, 2H, H_2O), 0.90 (s, 6H, Sn-CH_3). ^{13}C NMR (*d*-DMSO, ppm): 172.11 (COO), 162.3 (C=N), 154.6 (C^3), 147.4 (CONH), 135.2 (C^{10}), 129.6 (C^{11}), 129.4, 128.5 128.4, 127.4 126.5, 126.2, 125.3, 124.2 (aromatic carbons), 121.5 (C^7), 117.8 (C^2), 109.0 (C^4), 10.1 (Sn–CH_3).

4.4.2. n-$Bu_2Sn[3\text{-}HO\text{-}C_{10}H_6CON_2C(C_6H_5)CO_2]\cdot(C_2H_5OH)$ ***(2)***

Yield: 85 %, M.p.: 200-201℃. Anal. Calc. for $C_{29}H_{36}N_2O5Sn$: C, 56.98; H, 5.94; N, 4.58%; Found: C, 56.87; H, 5.58; N,4.32%. IR (KBr, cm^{-1}): 1639 (s, $\upsilon_{as}COO$); 1390 (s, υ_sCOO); 1579 (m, C=N-N=C); 546 (m, Sn-O); 525 (w, Sn-C); 476 (m, Sn-N). ^1H NMR ($CDCl_3$, δ ppm): 11.37 (s, 1H, Ar-OH), 8.64(s, 1H, H_1), 7.97-7.95(m, 2H), 7.84(d, 1H, J=8 Hz, H_8), 7.67-7.62(m, 5H), 7.47(t, 1H, J=6 Hz, H_6), 7.30(t, 1H, J=8 Hz, H_7). 1.85-1.79 (m, 2H, Sn-C^1H_2), 1.70-1.64 (m, 2H, -C^2H_2-), 1.44-1.35 (m, 2H, -C^3H_2-), 0.90 (t, 3H, -C^4H_3, J= 6.0 Hz). ^{13}C NMR ($CDCl_3$, δ ppm): 176.1 (COO), 163.7 (C=N), 156.0 (C^3), 151.5 (CONH)，137.9 (C^{10}), 132.6 (C^{11}), 132.3, 130.9, 129.3, 129.1，128.9, 128.6, 127.6, 126.5(aromatic carbons), 123.9 (C^7), 117.6 (C^2), 111.9 (C^4), 27.1(Sn-C^1H_2-), 26.6 (-C^2H_2-), 23.3 (-C^3H_2-), 13.6(-C^4H_3).

4.4.3. {$Ph_2Sn[3\text{-}HO\text{-}C_{10}H_6CON_2C(C_6H_5)CO_2]\ (C_2H_5OH)\}_2$ ***(3)***

Yield: 58%, M.p.: 254-255℃. Anal. Calc. for $C_{66}H_{56}N_4O_{10}Sn_2$: C, 60.86; H, 4.33; N, 4.30%;. Found: C, 60.89; H, 3.89; N,4.65%. IR (KBr, cm^{-1}): 1637 (s, $\upsilon_{as}COO$); 1386 (s, υ_sCOO); 1573 (m, C=N-N=C); 630 (s, Sn-O-Sn); 522 (w, Sn-C); 475 (m, Sn-N). ^1H NMR ($CDCl_3$, δ ppm): 10.86 (s, 2H, Ar-OH),

8.59(s, 1H, H_1), 7.73-7.71(m, 3H)，7.68-7.63(m, 4H), 7.41(d, 1H, J=8 Hz), 7.32-7.21(m, 11H), 7.09(t, 1H, J=8Hz), 7.01-6.98(m, 2H), 3.41(q, 2H, -OCH_2-, J=12 Hz), 1.59(s, 1H, R-OH), 1.25(t, 3H, J=6 Hz, -OCH_2-CH_3). ^{13}C NMR ($CDCl_3$, δ ppm): 176.0 (COO), 162.4 (C=N), 155.9 (C^3), 151.7 (CONH), 138.0 (C^{10}), 136.4(C-Sn), 135.4, 132.6, 131.8, 131.1, 130.2, 129.8, 129.3, 128.5, 128.3, 127.5, 126.4 (aromatic carbons), 124.0 (C^7), 117.2 (C^2), 112.0 (C^4), 58.7(-OCH_2-), 18.6 (-OCH_2-CH_3).

4.4.4. {(o-Cl-Bz)$_2$Sn[3-HO-$C_{10}H_6CON_2C(C_6H_5)CO_2$]$_2$($C_2H_5OH$)}$_2$ ***(4)***

Yield: 72%, M.p.: 243-244℃. Anal. Calc. for $C_{70}H_{60}Cl_4N_4Sn_2$: C, 62.91; H, 4.53; N, 4.19; Found:C, 62.89; H, 4.50; N, 4.22; IR (KBr, cm^{-1}): 1637 (s, υ_{as}COO); 1390 (s, υ_sCOO); 1574 (m, C=N-N=C); 634 (s, Sn-O-Sn); 526 (w, Sn-C); 474 (m, Sn-N). ^{1}H NMR ($CDCl_3$, δ ppm): 10.83 (s, 2H, Ar-OH), 8.20 (s, 1H, H_1), 7.78-7.73(m 3H), 7.64(d, 1H, J=8 Hz), 7.57-7.55(m 3H), 7.47(t, 1H, J=8 Hz), 7.31 (t, 1H, J=6 Hz), 7.24-7.20(m, 4H), 7.16(s, 1H, H_4), 7.02-6.99(m, 4H), 2.99 (s, 4H, ArCH_2Sn). ^{13}C NMR ($CDCl_3$, δ ppm): 175.0 (COO), 163.2 (C=N), 155.8 (C^3), 151.6 (CONH), 137.5(C^{10}), 134.2(C-Cl), 133.2(C^{11}), 132.6，132.3, 130.8, 129.5, 129.3, 129.0, 128.6, 128.5, 127.8, 127.5, 126.4(aromatic carbons), 123.8 (C^7), 117.2 (C^2), 111.6 (C^4), 29.7 (ArCH_2Sn).

4.4.5. {(o-F-Bz)$_2$Sn[3-OH-$C_{10}H_6CON_2C(C_6H_5)CO_2$]($C_2H_5OH$)}$_2$ ***(5)***

Yield: 71%, M.p.: 113-114 °C. Anal. Calc. for $C_{70}H_{60}F_4N_4O_{10}Sn_2$: C, 59.20; H, 4.55; N, 3.84; Found: C, 59.01; H, 4.34; N, 4.56%. IR (KBr, cm–1): 1636(s, υ_{as}COO); 1388(s, υ_sCOO); 1575(m, C=N-N=C); 633 (s, O-Sn-O); 525(w, Sn-C); 474 (m, Sn-N). ^{1}H NMR (*d*-DMSO, δ ppm): 11.76(s, 1H, -ArOH), 8.48(s, 1H, H_1), 7.88(d, 1H, J=8 Hz, H_8), 7.62(d, 1H, J=8 Hz, H_5), 7.43(t, 1H, J=8 Hz, H_6), 7.28(t, 1H, J=8 Hz, H_7), 7.00(s, 1H, H_4), 6.96(t, 2H, J=8 Hz, H_{13}) 7.36-7.37(m, 3H), 7.10-7.09(m, 2H), 6.86-6.81(m, 2H), 6.71-6.66(m, 4H), 3.52(q, 2H, -OCH_2-,J=8 Hz), 3.36(s, 1H, R-OH), 1.12(t, 3H, J=6 Hz, -OCH_2-CH_3), 2.98(s, 4H, ArCH_2Sn). ^{13}C NMR (*d*-DMSO, δ ppm): 172.5 (COO), 162.6 (C=N), 160.2(C-F), 154.9 (C^3), 147.8 (CONH), 135.5 (C^{10}), 129.7(C^{11}), 129.3, 128.4, 127.7, 126.7, 126.2, 125.7, 125.1, 125.0, 124.6, 122.2 (aromatic carbons), 121.8(C^7), 118.2(C^2), 109.2(C^4), 55.7(-OCH_2-), 17.4(-OCH_2-CH_3), 29.8 (ArCH_2Sn).

4.5. In vitro cytotoxic activity

Stock solutions of complexes **1, 3** and the ligand were dissolved in DMSO at a concentrations of 10 mg/ml and diluted by cell culture medium to various working concentration. To avoid DMSO toxicity, the concentration of DMSO was less than 0.1% (v/v) in all experiments.

Briefly, cells were seeded onto 96-well flat-bottom plates for 24 hours before treatment to allow attachment of cell to the wall of the plate, then fed with dilutions of each drug. The plates were incubated at 37□, 5% CO_2 for a period of 48 h. After 48 h, cells were fixed, washed, and stained with sulforhodamine B stain. Excess stain was washed out with acetic acid and attached stain was recovered with EDTA buffer. Color intensity was measured in an ELISA reader. The relation between surviving fraction and tested compound concentrations is plotted to get the survival curve of each tumor cell line after the cytotoxicity of the specified compound and IC_{50} (dose of the tested compound which reduces survival to 50%) were evaluated.

As for MTT assay, the procedure was performed by the methods reported in the literature [6]. MTT was added after exposed to organotin complexes for 48 h. 4 h later, the absorbance of the plates was read at 490 nm with a ELx808 Absorbance Microplate Reader (Bio-Tek Co., USA).

4.6. Fluorescence spectra

Ethidium bromide (EB) and ct-DNA were dissolved in 10 mmol L^{-1} trihydroxymethylaminomethane (tris)-HCl buffer solution and the ct-DNA concentration per nucleotide was determined by absorption spectroscopy using the molar absorption coefficient (6600 L mol^{-1} cm^{-1}) at 260 nm, while the EB concentration was calculated by the ratio of the mass to its molecular weight. The title compounds were dissolved in DMSO and the concentration was determined in the same way as EB. The organotin complexes were added to the solution containing 25 μmol L^{-1} ct-DNA and 3 μmol L^{-1} EB at different concentrations (0, 12.5, 25, 37.5, 50, 62.5 μM). After 2 h, fluorescence quenching spectra were recorded at 530-700 nm with all samples excited at 258 nm.

4.7. Protein binding studies

The stock solution of proteins (100 μM) was prepared by dissolving the solid BSA in 10 mM phosphate buffer (pH = 7.4) and stored at 4°C for further use. A concentrated stock solution of the compounds was prepared in DMSO at concentrations of 2.5×10^{-3} M and diluted by phosphate buffer. Titrations were done manually by using a trace syringe and the fluorescence spectra were recorded with excitation wavelength of BSA at 280 nm and the emission at 290-450 nm by keeping the concentration of BSA constant (1.0 μM) while varying the complex concentration from 0 to 10 μM at room temperature. For synchronous fluorescence spectra, the concentration of BSA was kept at 1.0 μM and the compounds of different concentrations were added and the spectra were measured at two different

$\Delta\lambda$ values (difference between the excitation and emission wavelengths of BSA), such as 15 and 60 nm.

5. Supplementary material

CCDC 919033 (for **1**), 919034 (for **2**), 919028 (for **3**), 919029 (for **4**) and 919030 (for **5**) contain the supplementary crystallographic data for this paper. These data can be obtained free of charge via http://www.ccdc.cam.ac.uk/conts/retrieving.html, or from the Cambridge Crystallographic Data Centre, 12 Union Road, Cambridge CB2 1EZ, UK; fax: (+44) 1223-336-033; or e-mail: deposit@ccdc.cam.ac.uk.

Acknowledgements

We acknowledge the National Natural Foundation of China (21105042) and the Natural Science Foundation of Shandong Province (ZR2011BM007, ZR2010BQ021, ZR2011BQ015) for financial support. And this work was supported by Shandong "Tai–Shan Scholar Research Fund".

References

[1]. M.A. Jakupec, M. Galanski, V.B. Arion, C.G. Hartinger, B.K. Keppler, Antitumour metal compounds: more than theme and variations, Dalton Trans., 2008 (2) 183-194.

[2]. P.J. Dyson, G. Sava, Metal-based antitumour drugs in the post genomic era, Dalton Trans., 2006 (16) 1929-1933.

[3]. G. Gasser, I. Ott, N. Metzler-Nolte, Organometallic anticancer compounds, J. Med. Chem., 2011 (54) 3-25.

[4]. M. Yousefi, M. Safari, M.B. Torbati, V.M. Kazemiha, H.Sanati, A. Amanzadeh, New mononuclear diorganotin(IV) dithiocarboxylates: synthesis, characterization and study of their cytotoxic activities, Appl. Organometal. Chem., 2012 (26) 438-444.

[5]. C.L. Ma, S.L. Zhang, R.F. Zhang, Chiral self-assembly of triorganotin complexes: syntheses, characterization,crystal structures and antitumor activity of organotin(IV) complexes containing (R)-(+)-methylsuccinic acid, (S)-(+)-methylglutaric acid and L-(-)-malic acid ligands, Polyhedron, 2012 (31) 478-485.

[6]. (a) H.D. Yin, C.H. Yue, M. Hong, J.C. Cui, Q.K. Wu, X.Y. Zhang, Synthesis, structural characterization and in vitro cytotoxicity of diorganotin (IV) diimido complexes, Eur. J. Med.Chem., 2012 (58) 533-542.

(b) M. Hong, H.D.Yin, X.Y. Zhang, Ch. Li, C.H. Yue, Sh. Cheng, Di- and tri-organotin(IV) complexes with 2-hydroxy-1-naphthaldehyde 5-chloro- 2-hydroxybenzoylhydrazone: synthesis, characterization and in vitro antitumor activities, J. Organomet. Chem., 2013 (724) 23-31.

[7]. D.B. Shpakovsky, C.N. Banti, G. Beaulieu-Houle, N. Kourkoumelis, M. Manoli, M.J. Manos, A.J. Tasiopoulos, S.K. Hadjikakou, E.R. Milaev, K. Charalabopoulos, T. Bakas, I.S. Butlerd, N. Hadjiliadisa, Synthesis, structural characterization and in vitro inhibitory studies against human breast cancer of the is-(2,6-di-tert-butylphenol)tin(IV) dichloride and its complexes, Dalton Trans., 2012(41) 14568-14582.

[8]. a) M. Gielen, A.G. Davies , K. Pannell , E. Tiekink, Tin chemistry: fundamentals, frontiers, and applications, J. Wiley & Sons, 2008.

b) M. Gielen, E.R.T. Tiekink, Metallotherapeutic drugs and metal-based diagnostic agents: the use of metals in medicine, J. Wiley & Sons, 2005.

[9]. A. Alama, M. Viale, M. Cilli, C. Bruzzo, F. Novell , B.Tasso, F. Sparatore, In vitro cytotoxic activity of tri-n-butyltin(IV)lupinylsulfide hydrogen fumarate (IST-FS 35) and preliminary antitumor, Invest New Drugs, 2009 (27) 124–130.

[10]. X.M. Shang, X.G. Meng, E.C.B.A. Alegria, Q.S. Li, M.F.C. Guedes da Silva, M.L. Kuznetsov, A.J.L. Pombeiro, Syntheses, molecular structures, electrochemical behavior, theoretical study, and antitumor activities of organotin(IV) complexes containing 1-(4-Chlorophenyl)-1-cyclopentanecarboxylato Ligands, Inorg. Chem., 2011 (50) 8158–8167.

[11]. X.M. Shang, N. Ding, G.Y. Xiang, Novel di-n-butyltin(IV) derivatives: synthesis, high levels of cytotoxicity in tumor cells and the induction of apoptosis in KB cancer cells, Eu.J. Med.Chem., 2012 (48) 305-312.

[12]. M. Nath, M. Vats, P. Roy, Tri- and diorganotin(IV) complexes of biologically important orotic acid: synthesis, spectroscopic studies, in vitro anti-cancer, DNA fragmentation, enzyme assays and in vivo anti-inflammatory activities our recent results with organotin(IV) species, Eu.J. Med.Chem., 2013 (59) 310-321.

[13]. M.V. Angelusiu, S.F. Barbuceanu, C.Draghici, G.L. Almajan, New Cu(II), Co(II), Ni(II) complexes with aroyl-hydrazone based ligand: synthesis, spectroscopic characterization and in vitroantibacterial evaluation, Eur. J. Med. Chem., 2010 (45) 2055–2062.

[14]. H.G. Aslan, S. Ozcan, N. Karacan, Synthesis, characterization and antimicrobial activity of salicylaldehyde benzenesulfonylhydrazone (Hsalbsmh) and its Nickel(II), Palladium(II), Platinum(II), Copper(II), Cobalt(II) complexes, Inorg. Chem. Commun., 2011(14) 1550–1553.

[15]. Z. Xu, X. Zhang, W. Zhang, Y. Gao, Z. Zeng, Synthesis, characterization, DNA interaction and antibacterial activities of two tetranuclear cobalt(II) and nickel(II) complexes with salicylaldehyde 2-phenylquinoline-4-carboylhydrazone, Inorg. Chem. Commun., 2011(14)1569–1573.

[16]. D.S. Kalinowski, D.R. Richardson, The evolution of iron chelators for the treatment of iron overload disease and cancer, Pharmacol. Rev., 2005(57) 547–583.

[17]. K.S. Putt, G.W. Chen, J.M. Pearson, J.S. Sandhorst, M.S. Hoagland, J.T. Kwon, S.K. Hwang, H. Jin, M.I. Churchwell, M.H. Cho, D.R. Doerge, W.G. Helferich, P.J. Hergenrother, Small-molecule activation of procaspase-3 to caspase-3 as apersonalized anticancer strategy, Nat. Chem. Biol., 2006 (2) 543−550.

[18]. Y. Yu, D.S. Kalinowski, Z. Kovacevic, A.R. Siafakas, P.J. Jansson, C. Stefani, D.B. Lovejoy, P.C. Sharpe, P.V. Bernhardt, D. R. Richardson, Thiosemicarbazones from the old to new: iron chelators that are more than just ribonucleotide reductase inhibitors, J. Med. Chem., 2009(52) 5271–5294.

[19]. D.R. Richardson, P.C. Sharpe, D.B. Lovejoy, D. Senaretne, D.S. Kalinowski, M. Islam, P.V. Bernhardt, Dipyridyl thiosemicarbazone chelators with potent and selective antitumor activity form iron complexes with redox activity, J. Med. Chem., 2006(49) 6510–6521.

[20]. J.Q. Tong, F.F.Tian, Q. Li, L.L. Li, C. Xiang, Y.Liu, J. Dai, F.L. Jiang, Probing the adverse temperature dependen ce in the staticfluorescence quenching of BSA induced by a novel anticancer hydrazone, Photochem, Photobiol. Sci., 2012(11) 1868-1879.

[21]. L. Alagesan, N.S.P. Bhuvanesh, N. Dharmaraj, Potentially cytotoxic new copper(II) hydrazone complexes: synthesis, crystal structure and biological properties, Dalton Trans., 2013(42) 7210-7223.

[22]. D.S. Raja, N.S.P. Bhuvanesh, K. Natarajan, A novel water soluble ligand bridged cobalt(II) coordination polymer of 2-oxo-1,2-dihydroquinoline-3-carbaldehyde (isonicotinic) hydrazone: evaluation of the DNA binding, protein interaction, radical scavenging and anticancer activity, Dalton Trans., 2012(41)4365-4377.

[23]. E.Ramachandran, D.S. Raja, N.S. P. Bhuvaneshb, K.Natarajan, Mixed ligand palladium(II) complexes of 6-methoxy-2-oxo-1,2-dihydroquinoline-3-carbaldehyde 4N-substituted thiosemicarbazones with triphenylphosphine co-ligand: Synthesis, crystal structure and biological properties, Dalton Trans., 2012(41) 13308-13323.

[24]. L.N. Wang, W.W. Qin, X.L. Tang, W. Dou, W.S Liu, Development and applications of fluorescent indicators for Mg^{2+} and Zn^{2+}, J. Phys. Chem., A 2011 (115) 1609-1616.

[25]. A. Kamal, R. Ramu, V. Tekumalla, G.B.R. Khanna, M.S. Barkume, A.S. Juvekar, S.M. Zingde, Bioorg. Med. Chem., 2007(15) 6868-6875.

[26]. H.D. Yin, H. Liu, M. Hong, Synthesis, structural characterization and DNA-binding properties of organotin(IV) complexes based on Schiff base ligands derived from 2-hydroxy-1-naphthaldy and 3- or 4-aminobenzoic acid, J. Organomet. Chem., 2012 (713) 1-9.

[27]. T.M. Sielecki, J.F. Boylan, P.A. Benfield, G.L. Trainor, Cyclin-dependent kinase inhibitors: useful targets in cell cycle regulation, J. Med. Chem., 2000(43) 1-18.

[28]. H.N. Hou, Z.D. Qi, Y.W. OuYang, F.L. Liao, Y. Zhang, Y. Liu, Studies on interaction between Vitamin B12 and human serum albumin, J. Pharm. Biomed. Anal., 2008 (47) 134-139.

[29]. P. Sathyadevi, P. Krishnamoorthy, R.R. Butorac, A.H. Cowley, N. Dharmaraj, Synthesis of novel heterobimetallic copper(I) hydrazone Schiff base complexes: a comparative study on the effect of heterocyclic hydrazides towards interaction with DNA/protein, free radical scavenging and cytotoxicity, Metallomics, 2012(4) 498-511.

[30]. (a) C. Vatsa, V.K. Jain, T.K. Das, E.R.T. Tiekink, Structural chemistry of organotin carboxylates VI. Characterization of $\{[R_2Sn(O_2CR')]_2O\}_2$ (R = Me, Et, *n*-Pr and *n*-Bu; R´ = thiophene and furan). X-ray crystal structure of $\{[n\text{-}Bu_2Sn(O_2CC_4H_3S)]_2O\}_2$, J. Orgunornet. Chem., 1990 (396) 9-18.

(b) H.D. Yin, M. Hong, H.L. Xu, Z.J. Gao, G. Li, D.Q. Wang, Self-assembly of organotin(IV) moieties with the Schiff-Base ligands pyruvic acid Isonicotinyl hydrazone and pyruvic acid salicylhydrazone: synthesis, characterization, and crystal structures of monomeric or polymeric complexes, Eur. J. Inorg. Chem., 2005 (22) 4572-4581.

[31]. H.D. Yin, M. Hong, Q.B. Wang, S.C. Xue, D.Q. Wang, Synthesis and structural characterization of diorganotin(IV) esters with pyruvic acid isonicotinyl hydrazone and pyruvic acid salicylhydrazone Schiff bases, J. Organomet. Chem. 2005 (690) 1669-1676.

[32]. Z.A. Siddiqi, M. Shahid, S. Kumar, M. Khalid, S. Noor, Synthesis, crystal structure and in vitro antitumor activity of carboxylate bridged dinuclear organotin(IV) complexes, J. Organomet. Chem., 2009 (694) 3768–3774.

[33]. T.S. Basu Baul, W. Rynjah, E. Rivarola, C. Pettinari, A. Linden, Synthesis and characterization of the first diorganotin(IV) complexes containing mixed arylazobenzoic acids and having skew trapezoidal bipyramidal geometry, J. Organomet. Chem., 2005 (690) 1413-1421.

[34]. H.N. Dogan, A. Duran, S. Rollas, G. Sener, M.K. Uysalb, D.Gülen. Synthesis of new 2,5-disubstituted-1,3,4-thiadiazoles and preliminary evaluation of anticonvulsant and antimicrobial activities, Bioorg. Med. Chem., 2002 (10) 2893–2898 .

[35]. S. Sylvestre, K. Pandiarajan, NMR spectral study of some 2r,6c-diarylpiperidin-4-one (3'-hydroxy-2'-naphthoyl)hydrazones with special reference to γ-syn effect, Spectrochim. Acta, Part A, 2011 (78) 153–159.

[36]. H.D. Yin, C.H. Wang, Y. Wang, C.L. Ma, J.X. Shao, Synthesis and structure of seven-coordinate dimmer $\{(PhCH_2)_2Sn[2,6\text{-}(O_2C)_2C_5H_3N](CH_3OH)\}_2$, Chem. J. Chin. Univ., 2003 (24) 68–72.

[37]. Z.Y. Yang, R.D. Yang, K.B. Yu, The crystal structures and thermal stability of the complexes of 2-Oxo-propionic acid (4-pyridinecarbony1) hydrazone with alkaline earth metals. Chim. Acta Chim. Sin., 1999 (57) 236-243.

[38]. S.Y. He, W.K. Cao, J.L. Chen, J.S. Zhao, Q.Z. Shi, R.X. Wang, J. Sun, Synthesis，crystal structure and antibacterial activity of copper(II) complexes with 2-oxo-propionic acid salicyloyl hydrazon, Chem. J. Chin. Univ., 2002 (23) 991-995.

[39]. L.R. Reverte, E.C. Garcia, J.C.Torres, S. Prashar, G.N. Kaluderović, J.A. Ferragut, S.G. Ruiz, Study of the anticancer properties of tin(IV) carboxylate complexes on a panel of human tumor cell lines, Chem. Med. Chem., 2012 (7) 301 – 310.

[40]. J. Marmur, A procedure for the isolation of deoxyribonucleic acid from micro-organisms, J. Mol. Biol., 1961 (3) 208-218.

[41]. M. Ghaderi, S.Z. Bathaie, A.A. Saboury, H. Sharghi, S.Tangestaninejad, Interaction of an Fe derivative of TMAP (Fe(TMAP)OAc) with DNA in comparison with free-base TMAP, Int. J. Biol. Macromol., 2007 (41) 173-179.

[42]. B.C. Baguley, M. Le Bret. Quenching of DNA-ethidium fluorescence by amsacrine and other antitumor agents: a possible electron-transfer effect, Biochemistry, 1984 (23) 937-943.

[43]. J.R. Lakowicz, G. Webber, Quenching of fluorescence by oxygen. probe for structural fluctuations in macromolecules, Biochemistry, 1973 (12) 4161-4170.

[44]. M.R. Eftink , C.A. Ghiron, Fluorescence quenching of indole and model micelle systems, J. Phys. Chem., 1976, (80) 486-493.

[45]. W.R. Ware, Oxygen quenching of fluorescence in solution: an experimental study of the diffusion progress, J. Phys. Chem., 1962 (66) 455-458.

[46]. J.H. Tang, F. Luan, X.G. Chen, Binding analysis of glycyrrhetinic acid to human serum albumin: fluorescence spectroscopy, FTIR, and molecular modeling, Bioorg. Med. Chem., 2006 (14) 3210−3217.

[47]. K. Sisido, Y. Takeda, Z. Kinugawa, Direct synthesis of organotin compounds: di- and tribenzyltin chlorides, J Am. Chem. Soc., 1961 (83) 538–541.

Scheme Captions

Scheme 1. The reaction procedures.

Figure Captions

Fig. 1. Crystal structure of complexes **1**, **3**, **4** and **5** (hydrogen atoms are omitted for clarity). Atoms drawn at 30% probability.

Fig. 2. Crystal structure of complex **2** (hydrogen atoms are omitted for clarity). Atoms drawn at 30% probability.

Fig. 3. Effects of complexes **1** (A) and **3** (B) on the fluorescence spectra of EB-DNA system, respectively. [DNA] = 25 μmol·L^{-1}, [EB] =3 μmol·L^{-1}, from 1 to 6, [VOL]/[DNA] = 0, 0.5, 1.0, 1.5, 2.0, 2.5, respectively; Inset: plot of I_0/I vs. r (r = [VOL]/[DNA]). λ_{ex} = 258 nm.

Fig. 4. Effects of complex **3** on the fluorescence (A) and synchronous spectra of BSA system (B, C). [BSA] = 1.0 μM, from 1 to 9, [VOL] = 0, 1.25, 2.5, 3.75, 5.0, 6.25, 7.5, 8.75, 10 μM , respectively. $\Delta\lambda$ = 60 nm (B) and $\Delta\lambda$ = 15 nm (C), λ_{ex} = 280 nm.

Fig. 5. Stern–Volmer plots (A) and Scatchard plots (B) of the fluorescence titration of complexes **1** and **3** with BSA.

Fig. S1. Absorption spectra of complexes **1**(e), **2**(d), **3**(f), **4**(a) and **5**(b) and the ligand(c) at 1×10^{-4} M in DMSO.

Fig. S2. Effects of complex **1** on the fluorescence(A) and synchronous spectra of BSA system. [BSA] = 1.0 μM, from 1 to 9, [VOL] = 0, 1.25, 2.5, 3.75, 5.0, 6.25, 7.5, 8.75, 10 μM , respectively. $\Delta\lambda$ = 60 nm (B) and $\Delta\lambda$ = 15 nm (C), λ_{ex} = 280 nm.

Table Captions

Table 1. Crystal data and structure refinement parameters for complexes **1-5.**

Table 2. Selected bond lengths (Å) and angles (°) for complexes **1**, **3**, **4** and **5.**

Table 3. Selected bond lengths (Å) and angles (°) for complex **2**

Table 4. Hydrogen bonding geometries for complexes **1-5.**

Table 5. Half maximal inhibitory concentration (ug/ml) of complexes **1**, **3** and the ligand against tumor cell lines (n=3)..

Table 6. The quenching constant, binding constant and number of binding sites for the interactions of complexes **1** and **3** with BSA.

Table1. Crystal data and structure refinement parameters for complexes **1-5**

Complex	**1**	**2**	**3**	**4**	**5**
Empirical formula	$C_{42}H_{40}N_4O_{10}Sn_2$	$C_{29}H_{36}N_2O_5Sn$	$C_{66}H_{56}N_4O_{10}Sn_2$	$C_{70}H_{60}Cl_4N_4O_{10}Sn_2$	$C_{70}H_{60}F_4N_4O_{10}Sn_2$
Formula weight	998.16	611.29	1302.53	1496.40	1430.60
Wavelength (Å)	0.71073	0.71073	0.71073	0.71073	0.71073
Crystal system	Monoclinic	Triclinic	Triclinic	Monoclinic	Monoclinic
Space group	$P2_1/C$	P_{-1}	P_{-1}	$P2_1/C$	$P2_1/C$
a (Å)	7.3461(6)	9.1890(10)	11.6700(12)	14.8371(16)	14.9860(15)
b (Å)	19.9138(10)	10.1621(11)	12.4841(14)	11.1193(11)	10.8631(9)
c (Å)	13.8773(11)	15.9512(17)	12.7469(13)	19.7634(18)	20.179(2)
α (º)	90	100.576(2)	61.2340(10)	90	90
β (º)	97.2290(10)	93.6980(10)	66.1330(10)	96.034(2)	96.7490(10)
γ (º)	90	91.5290(10)	88.998(2)	90	90
V (Å^3)	2014.0(3)	1460.0(3)	1451.9(3)	3242.5(6)	3262.2(6)
Z	4	2	1	2	2
Dcalc (Mg/m^3)	1.296	1.390	1.490	1.533	1.456
μ (mm^{-1})	1.296	0.913	0.924	0.998	0.838
F(000)	988	628	660	1512	1448
Crystal size (mm)	0.49 x 0.45 x 0.20	0.49 x 0.48 x 0.37	0.45 x 0.30 x 0.18	0.49 x 0.47 x 0.47	0.30 x 0.18 x 0.14
Reflections collected	8946	7576	7600	15992	15754
Unique reflections [R_{int}]	3536 [R(int)=0.0603]	5063 [R(int)=0.0201]	5037 [R(int)=0.0196]	5713 [R(int)= 0.0321]	5736 [R(int)= 0.0447]
Data/restraints/parameters	3536 / 0 / 264	5063 / 494 / 338	5037 / 6 / 374	5713 / 0 / 407	5736 / 0 / 501
Goodness-of-fit on F^2	1.037	1.072	1.125	1.089	1.060
Final *R* indices [I>2σ (I)]	R_1 = 0.0416 wR_2 = 0.0965	R_1 = 0.0506 wR_2= 0.1227	R_1 = 0.0329 wR_2 = 0.0633	R_1 = 0.0358 wR_2 = 0.0811	R_1 = 0.0505 wR_2 = 0.1025
R indices (all data)	R_1 = 0.0631 wR_2 = 0.1090	R_1 = 0.0807 wR_2 = 0.1547	R_1 = 0.0491, wR_2 = 0.0734	R_1 = 0.0616 wR_2 = 0.1002	R_1 = 0.0928 wR_2 = 0.1301

Table 2. Selected bond lengths (Å) and angles (°) for complexes **1, 3, 4** and **5**

Complex	**1**	**3**	**4**	**5**
Sn(1)-O(3)	2.216(3)	2.182(2)	2.162(3)	2.181(4)
Sn(1)-N(1)	2.299(4)	2.294(3)	2.244(3)	2.274(5)
Sn(1)-O(1)	2.361(3)	2.361(2)	2.349(3)	2.393(4)
Sn(1)-O(5)	2.373(3)	2.315(2)	2.428(3)	2.417(5)
Sn(1)-O(1)#1	2.661(3)	2.581(2)	2.628(3)	2.638(4)
N(2)-C(9)	1.345(5)	1.331(4)	1.332(5)	1.339(8)
O(3)-C(9)	1.270(5)	1.274(4)	1.278(5)	1.287(7)
N(1)-C(2)	1.292(5)	1.293(4)	1.290(5)	1.294(7)
O(1)-C(1)	1.280(5)	1.282(4)	1.287(5)	1.289(7)
O(2)-C(1)	1.238(5)	1.234(4)	1.232(5)	1.245(7)
O(3)-Sn(1)-N(1)	69.45(11)	69.54(8)	70.71(11)	70.56(16)
N(1)-Sn(1)-O(1)	68.42(12)	68.34(8)	68.94(11)	68.49(15)
O(3)-Sn(1)-O(5)	75.98(11)	76.05(8)	75.26(11)	75.99(16)
O(1)-Sn(1)-O1#1	66.56(10)	67.71(8)	65.12(10)	65.58(15)
O(5)-Sn(1)-O1#1	79.60(10)	78.37(7)	79.94(10)	79.41(15)
C(20)-Sn(1)-C(21)	166.0(2)			
C(20)-Sn(1)-C(26)		171.66(13)		
C(20)-Sn(1)-C(27)			161.85(18)	163.2(3)

Symmetry transformations used to generate equivalent atoms: Complex **1**: -x, 1-y, 1-z; Complex **3**: -x+2, -y+1, -z;

Complex **4**: -x, -y, -z+1; Complex **5**: -x+1, -y+1, -z;

Table 3. Selected bond lengths (Å) and angles (°) for complex **2**

Complex 2			
Sn(1)-O(3)	2.175(4)	O(3)-C(9)	1.288(7)
Sn(1)-N(1)	2.257(5)	N(1)-C(2)	1.290(8)
Sn(1)-O(1)	2.304(4)	O(1)-C(1)	1.275(7)
Sn(1)-O(5)	2.415(5)	O(2)-C(1)	1.232(8)

Sn(1)-C(24)	2.107(9)	Sn(1)-C(20)	2.119(8)
N(2)-C(9)	1.324(8)	O(3)-Sn(1)-N(1)	70.06(16)
N(1)-Sn(1)-O(1)	69.65(15)	O(3)-Sn(1)-O(5)	78.95(16)
C(20)-Sn(1)-C(24)	162.5(4)		

Table 4. Hydrogen bonding geometries for complexes **1**-**5**

D-H...A	d(D-H)	d(H···A)	d(D···A)	<(DHA)
1				
O(5)-H(5B)···O(4)#1	0.85	1.96	2.799(5)	167.7
O(5)-H(5A)···O(2)#2	0.85	1.81	2.656(4)	174.2
O(4)-H(4)···N(2)	0.82	1.85	2.573(5)	146.9
C(10)-H(10)···O(3)	0.93	2.46	2.788(5)	100.6
2				
O(4)-H(4)···N(2)	0.82	1.90	2.615(6)	145.4
O(5)-H(5)···O(2)#1	0.82	1.82	2.619(7)	166.4
C(10)-H(10)···O(3)	0.93	2.42	2.759(8)	101.6
3				
O(4)-H(4)···N(2)	0.82	1.85	2.580(4)	146.9
O(5)-H(5)···O(2)#1	0.85	1.75	2.589(3)	167.9
O(5)-H(5)···O(1)#1	0.85	2.65	3.101(3)	114.5
4				
O(4)-H(4)···N(2)	0.82	1.83	2.563(5)	147.3
O(5)-H(5)···O(2)#1	0.82	1.86	2.628(5)	156.2
5				
O(4)-H(4)···N(2)	0.82	1.85	2.579(7)	147.1
O(5)-H(5)···O(2)#1	0.82	1.83	2.628(7)	163.2

Symmetry code: (#1 for **1)** x, -y+3/2, z-1/2; (#2 for 1) -x, -y+1, -z+1; (#1 for **2**) -x+1, -y+2, -z; (#1 for **3**) -x+2, -y+1, -z; (#1 for **4**) -x, -y, -z+1; (#1 for **5**) -x+1, -y+1, -z;

Table 5. Half maximal inhibitory concentration (ug/ml) of complexes **1**, **3** and the ligand against tumor cell lines (*n*=3).

Complex	IC_{50} (ug/ml)					
	SRB				MTT	
	SMMC-7721	A549	P388	WiDr	HCT-116	A549
1	21.96±1.20	29.45±0.30	24.46±0.37	12.48±0.50	16.94	30.36
3	8.47±0.70	20.19±3.16	12.37±3.12	17.58±0.33	4.00	18.32
Ligand	>100	>100	>100	>100	>100	>100
cisplatin	--	--			53	>60

Table 6. The quenching constant, binding constant and number of binding sites for the interactions of complexes **1** and **3** with BSA.

Compound	Ksv	Kq	n	K_{bin}
1	1.0877×10^{5}	1.0877×10^{13}	1.237	1.72×10^{6}
3	1.0301×10^{5}	1.0301×10^{13}	1.162	6.82×10^{5}

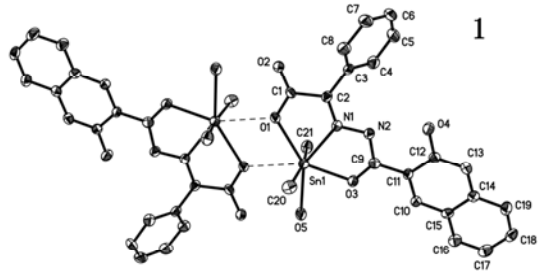

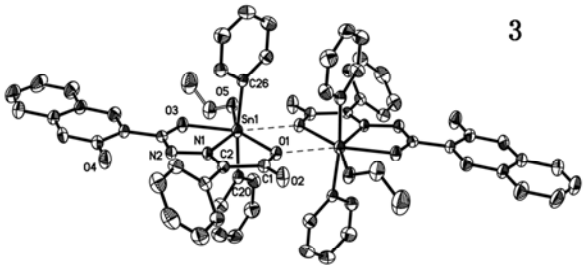

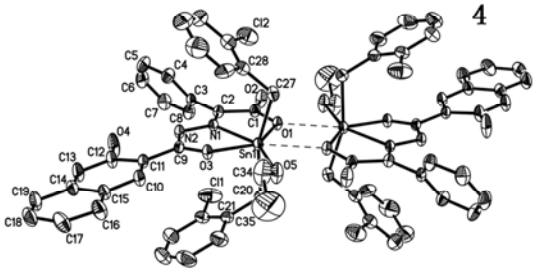

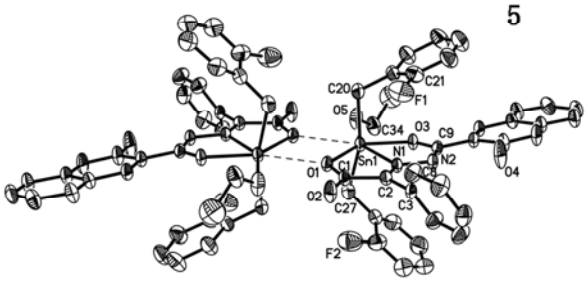

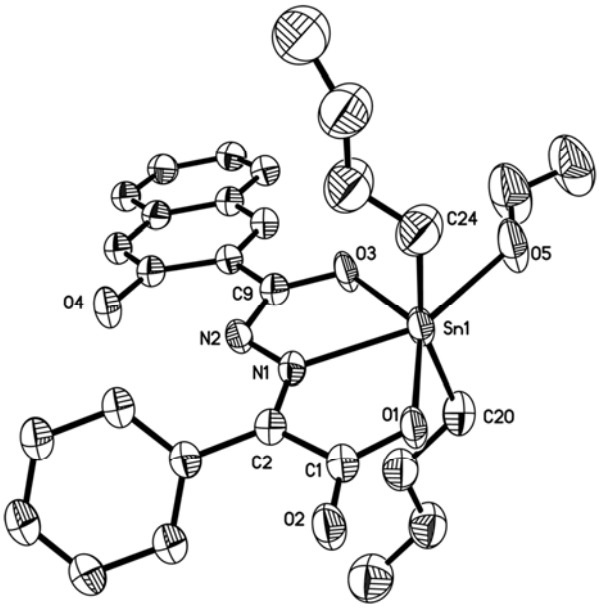

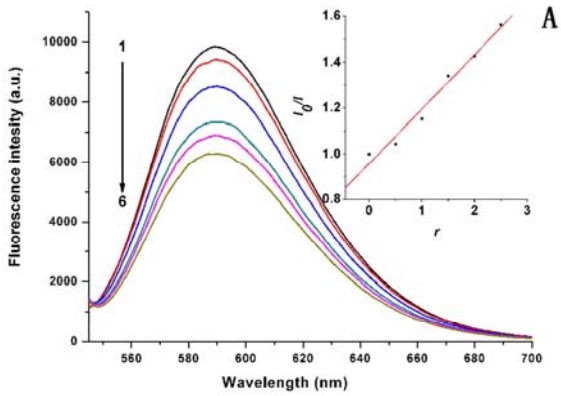

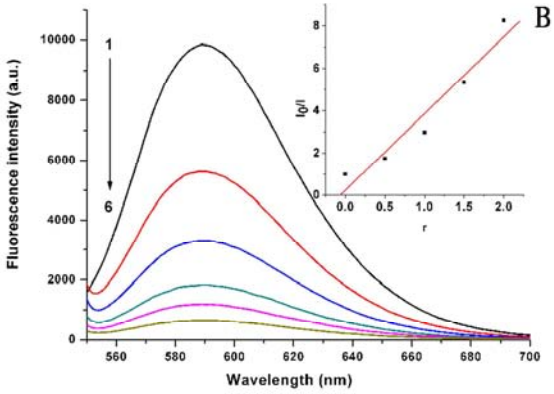

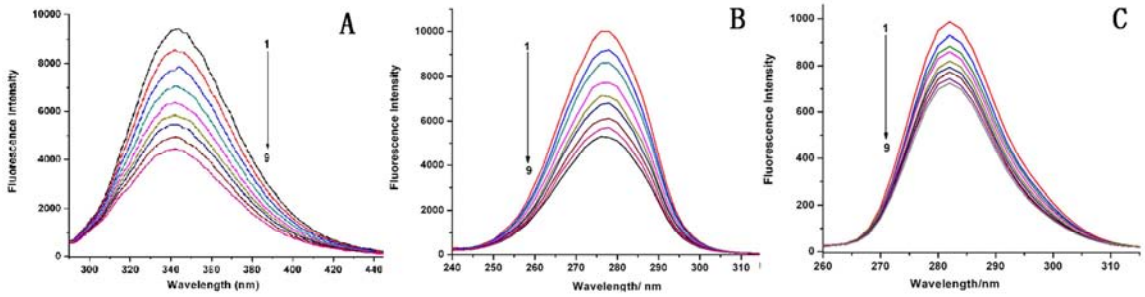

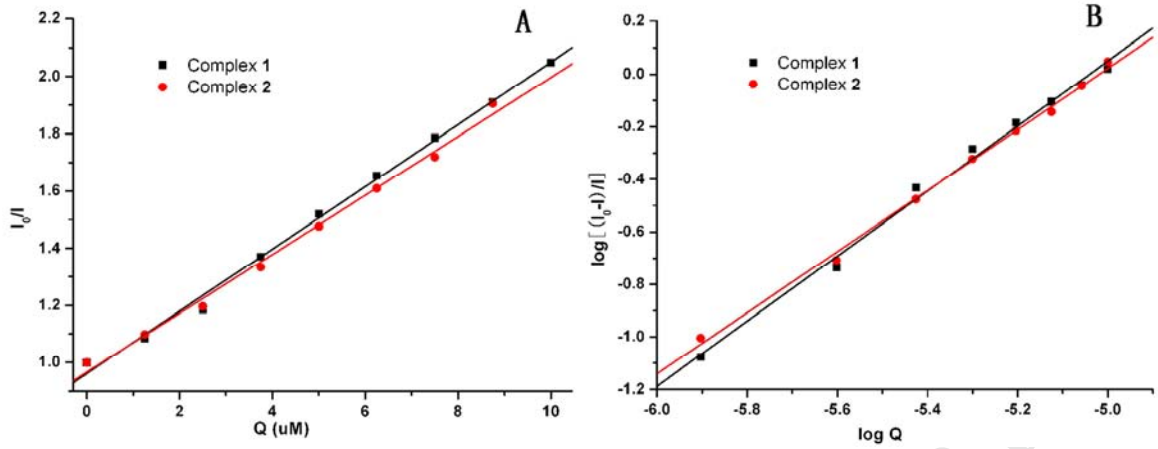

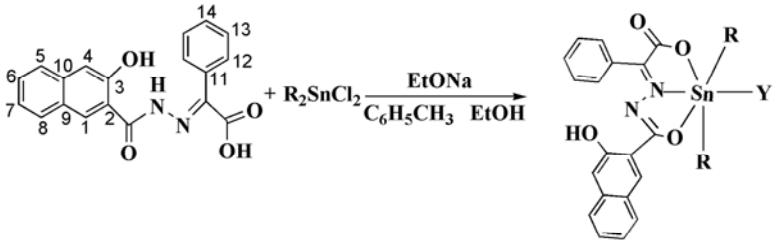

R =*n*-Bu Y=CH_3CH_2OH 2

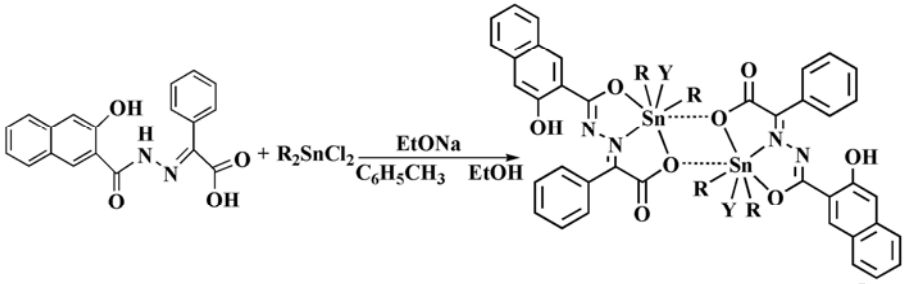

R = CH_3 Y=H_2O 1

Ph Y=CH_3CH_2OH 3

o-ClBz Y=CH_3CH_2OH 4

o-FBz Y=CH_3CH_2OH 5